Drug Design, Development and Therapy Dovepress

Open Access Full Text Article ORIGINAL RESEARCH

Effects of Oltipraz on the Glycolipid Metabolism and the Nrf2/HO-1 Pathway in Type 2 Diabetic Mice

Yunfei Luo[1,*], Shaohua Sun[1,2,*], Yuying Zhang[1,*], Shuang Liu[1], Haixia Zeng[1], jin-E Li[1], Jiadian Huang[1], Lixuan Fang[1], Shiqi Yang[1], Peng Yu[1], Jianping Liu[1,3,4]

[1]Department of Endocrinology and Metabolism of the Second Affiliated Hospital, Jiangxi Medical College, Nanchang University, Nanchang, Jiangxi, 330031, People's Republic of China; [2]Department of Metabolism and Endocrinology, XinSteel Center Hospital, Xinyu, Jiangxi, 338000, People's Republic of China; [3]Institute for the Study of Endocrinology and Metabolism in Jiangxi Province, Nanchang, Jiangxi, 330031, People's Republic of China; [4]Branch of National Clinical Research Center for Metabolic Diseases, Nanchang, Jiangxi, 330031, People's Republic of China

*These authors contributed equally to this work

Correspondence: Jianping Liu, The Second Affiliated Hospital, Jiangxi Medical College, Nanchang University, No. 1, Minde Road, Nanchang, Jiangxi, 330031, People's Republic of China, Email ndefy14105@ncu.edu.cn

Purpose: Oltipraz has various applications, including for treating cancer, liver fibrosis, and cirrhosis. However, its role in regulating metabolic processes, inflammation, oxidative stress, and insulin resistance in STZ-induced T2DM remains unclear. Hence, a comprehensive understanding of how oltipraz ameliorates diabetes, particularly inflammation and oxidative stress, is imperative.

Methods: The negative control (NC), T2DM model (T2DM), and T2DM models treated with oltipraz (OLTI) and metformin (MET) were constructed. The RNA sequencing (RNA-Seq) was performed on the pancreatic tissues. H&E staining was conducted on the liver and pancreatic tissues. The intraperitoneal glucose tolerance test (IPGTT), blood glucose and lipids, inflammatory factors, and oxidative stress indexes were measured. qPCR and Western blotting examined the nuclear factor erythroid-derived 2-like 2 (Nrf2)/hemoglobin-1 (HO-1) signaling pathway, cell apoptosis-related genes, and Reg3g levels. Immunofluorescence (IF) analysis of the pancreas was performed to measure insulin secretion.

Results: A total of 256 DEGs were identified in OLTI_vs_T2DM, and they were mainly enriched in circadian rhythm, cAMP, AMPK, insulin, and MAPK signaling pathways. Moreover, Reg3g exhibits reduced expression in T2DM_vs_NC, and elevated expression in OLTI_vs_T2DM, yet remains unchanged in MET_vs_T2DM. OLTI reduced fasting blood glucose and alleviated T2DM-induced weight loss. It improved blood glucose and insulin resistance, decreased blood lipid metabolism, reduced inflammation and oxidative stress through the Nrf2/HO-1 signaling pathway, mitigated pancreatic and liver tissue injury, and enhanced pancreatic β-cell insulin secretion. OLTI exhibited anti-apoptosis effects in T2DM. Moreover, OLTI exhibits superior antioxidant activity than metformin.

Conclusion: In summary, OLTI improves blood glucose and insulin resistance, decreases blood lipid metabolism, reduces inflammation and apoptosis, suppresses oxidative stress through the Nrf2/HO-1 signaling pathway, mitigates pancreatic and liver tissue injury, and enhances pancreatic β-cell insulin secretion, thereby mitigating T2DM symptoms. Moreover, Reg3g could be an important target for OLTI treatment of T2DM.

Keywords: Oltipraz, T2DM, oxidation stress, Nrf2, inflammation

Introduction

Diabetes mellitus (DM) is a disease characterized by metabolic disorders and chronic inflammation,[1] which is divided into type 1 diabetes mellitus (T1DM) and type 2 diabetes mellitus (T2DM) according to their pathological characteristics. T2DM accounts for 90–95% of all the DM patients.[2] The incidence of T2DM is associated with genetic factors, dietary patterns, age, and lifestyle, accompanied by graded insulin resistance and pancreatic β-cell dysfunction.[3,4] The occurrence of T2DM is closely related to inflammation, oxidative stress, and apoptosis. Elevated blood glucose caused by DM instigates inflammation, releasing inflammatory cytokines such as interleukin (IL-6), and tumor necrosis factor-α (TNF-α), exacerbating pancreatic β-cell inflammation and insulin resistance.[5] This inflammatory indicators have demonstrated

Received: 5 July 2024
Accepted: 26 November 2024
Published: 5 December 2024

association with adipose tissue and implicate them in insulin resistance development. The suppression of systemic inflammation can consequently alleviate symptoms of oxidative stress characteristic in T2DM.[6] Oxidative stress is considered one of the significant risk factors for T2DM.[7] When DM patients endure prolonged hyperglycemia, the body oxidative stress increases leading to mitochondrial malondialdehyde (MDA) and reactive oxygen species (ROS) overproduction, and cell cytotoxicity.[8] ROS can activate nuclear factor-κB (NF-κB) and regulate downstream inflammatory factors, further amplifying cell inflammation. Additionally, ROS can stimulate Caspase-3 and Bax expression, suppress Bcl-2, and contribute to cell apoptosis.[9] Moreover, overexpression of Reg3g in pancreatic islets activates the Janus kinase 2/signal transducer and activator of transcription 3/NF-κB signaling, promoting β cell regeneration.[10] Reg3g notably alleviates β-cell dysfunction by restoring mitochondrial function via pSTAT3 (Ser727).[11] Therefore, deep studies on inflammation, oxidative stress, and cell apoptosis are pivotal for T2DM therapy.

DM prevention and treatment mainly depend on diet management and appropriate exercise. Oral therapies for T2DM patients include biguanides, sulfonylureas, thiazolidinediones, alpha-glucosidase inhibitors, glucagon-like peptide-1 receptor agonists (GLP-1RAs), and dipeptidyl peptidase IV inhibitors (DPPIVs).[12] However, these single-target drugs mainly manage blood glucose and delay-related complications. They fail to address DM completely for they only focused on reducing glucose but the real pathogen-insulin resistance. Therefore, the development of therapeutic drugs that enhance insulin resistance is crucial for DM treatment.

Oltipraz (OLTI) represents an effective Nrf2 agonist, demonstrating analgesic, antioxidant, and anti-inflammatory effects in various diseases including cancer, liver fibrosis, and cirrhosis.[13–16] OLTI mitigates high glucose-induced oxidation stress reaction and cell apoptosis via an antioxidant signaling pathway.[17] Nrf2's downstream targets, namely glutathione S-transferases, haem oxygenase-1 (HO-1), and superoxide dismutase (SOD), enhance insulin sensitivity.[18] Furthermore, Nrf2 suppresses inflammatory signals and endoplasmic reticulum stress.[19] Nrf2 interaction with the antioxidant response element (ARE) triggers an array of antioxidant reactions, specifically SOD, CAT, glutathione, NADPH, and HO-1, to combat oxidative stress by diminishing excess ROS, thus maintaining cell balance under diverse stimuli. Activation of the Nrf2/ARE pathway mitigates oxidative stress and IR in T2DM.[20] Evidence suggests that OLTI enhances the endogenous antioxidant activity of Nrf2, preventing obesity and insulin resistance caused by a high-fat diet,[21] enhancing the activity of the Nrf2/HO-1 signaling pathway, and reducing ROS expression and oxidative stress. Initial investigations showed that Oltipraz enhances Phase I and II enzyme activities, including GSTs, NQO1, microsomal epoxide hydrolase, aflatoxin aldehyde reductase, glucuronosyl transferases, as well as glutathione metabolism-enhancing enzymes such as glutathione reductase and glucose-6-phosphate dehydrogenase. The metabolic enzyme induction by Oltipraz is attributed to Nrf2/ARE. Moreover, Oltipraz modulates the expression and function of certain cytochrome P450 enzymes, specifically inducing Cyp2b10 via the activation of Nrf2.[22] OLTI exhibits a potent antioxidant effect on acute liver injury, heart failure, and kidney damage.[23] However, its role in regulating glucose and lipid metabolism, inflammation, oxidation, and insulin resistance in T2DM remains understudied.

In our present study, we examined the role of OLTI in regulating glucose and lipid metabolism, inflammation, oxidative stress, and insulin resistance in T2DM. Additionally, we compared these functions with MET. MET, a safe and efficacious anti-hyperglycemic agent, is a first-line oral medication for T2DM. It exerts beneficial effects by reducing oxidative stress and upregulating Nrf2.[24,25] The aim of this study was to elucidate the comprehensive function of OLTI in T2DM, and contrast its therapeutic effects with MET.

Materials and Methods

Animal Experiments

Thirty-two specific-pathogen-free male C57BL/6J mice, aged eight weeks and weighing 20–25g, were acquired from the Hunan SJA Laboratory Animal Co., Ltd (Changsha, China). Pursuing statistics and to accommodate future tissue requirements or to prevent unexpected mouse deaths, we maintained eight mice per group. The mice were randomly assigned to four groups: Control (NC group, n=8), T2DM (T2DM group, n=8), metformin-treated T2DM (MET group, n=8), oltipraz-treated T2DM (OLTI group, n=8). For T2DM, MET, and OLTI groups, the animals were fed with a high-fat diet for eight weeks (mice aged 111 days) and then received three intraperitoneal injections of 60mg/kg of STZ three times to establish the T2DM model.

To evaluate the T2DM model, fasting blood glucose (FBG) was measured at 1, 3, and 7 days after STZ injection, and over 11.1mmol/L was used as the threshold for successful model establishment. At 116 days, sixteen T2DM model animals were randomly selected and treated with oltipraz or metformin. Oltipraz was given orally at 0.2mL (150mg/kg) every other day, while metformin was given orally at 0.2mL (200mg/kg) every other day. NC and T2DM groups received with normal water. Treatments continued for four weeks. Mice were housed in separate cages under room temperatures with a 12 h:12 h light/dark cycle and free access to food and water. All animal experiments were approved by the Nanchang University Experimental Animal Ethics Committee (Protocol number: NCDXSYDWFL-2023127). In the whole experiment, FBG and weight were monitored every five days.

Mice were fasted for 12 hours prior to sampling, anesthetized with isoflurane, blood was collected, and the mice were euthanized. The liver and pancreas tissues were excised and either fixed or stored at −80 °C for subsequent experiments.

Intraperitoneal Glucose Tolerance Test (IPGTT)

The IPGTT was measured at the end of the experiments. Mice were fasted for 12 hours and FBG level was measured. Then, glucose solution (60mg/kg) was intra-abdominally injected, and blood glucose assessments were performed and recorded at 30, 60, 90, and 120 minutes.

Enzyme-Linked Immunosorbent Assay (ELISA)

ELISA analyses were performed on the serum samples from four groups using commercial kits. Fasting serum insulin, C-peptide, TNF-α, IL-6, IL-1β, and ROS levels were quantified. OD values were measured under one Microplate Reader (American Molecular Devices Company). The HOMA-IR index was calculated as fasting serum insulin×FBG/22.5.

TG, TC, HDL-C, and LDL-C Measurements

Serum was centrifuged at 3000rpm for 20 minutes and the supernatant was collected. Analysis of TC, TG, HDL-C, and LDL-C were performed on the PBC22A Plus fully automatic biochemical analyzer.

Hematoxylin-Eosin (H&E) Staining

The livers and pancreatic tissue from NC, T2DM, MET, and OLTI were collected, preserved in pre-cooled heparinized physiological saline and 4% paraformaldehyde, paraffin-embedded, and sectioned at 4μm, then subjected to H&E staining using an H&E staining kit (Solarbio, China) according to the manufacturer's instructions. NAFLD Activity Score (NAS) is a summation of scored steatosis (0–3), lobular inflammation (0–3), and hepatocellular ballooning (0–2).[26] The total islet area was quantified employing ImageJ software.

Immunofluorescence (IF) Analysis

Pancreatic sections were dehydrated and fixed with cold acetone for 10–20 mins at 4°C. Post-wash with PBST, they were serum-fixed at room temperature for 30 minutes before insulin (1:300, ET1601-12, huabio) primary antibodies were applied at 4 °C for 12h. Subsequently, the HRP-conjugated goat anti-rabbit IgG secondary antibody (1:20,000, BA1054, Boster) was incubated at 37°C for 30 minutes. Following this, the sections were washed, sealed with glycerin buffer (contained DAPI), and observed under the fluorescent microscope. Quantification was performed using ImageJ.

Glutathione Peroxidase (GSH-Px), Malondialdehyde (MDA), and Superoxide Dismutase (SOD) Measurements

Pancreatic tissue (0.4g) was shredded to obtain fiber-free substances. This was then centrifuged at 3600rpm for 10 minutes at 4°C. The supernatant was utilized for measuring the enzyme activities of glutathione peroxidase (GSH-Px) (A005-12-2), malondialdehyde (MDA) (A003-1-2), and superoxide dismutase (SOD, A001-1-2) using commercial kits obtained from Nanjing Jiancheng Bioengineering Institute (Nanjing, China).

Real-Time Quantitative PCR (qPCR)

The expression levels of Nrf2, HO-1, NQO1, Bax, Bcl-2, Caspase-3, Reg3g, and GAPDH were evaluated in pancreatic tissue. Total RNA was extracted using TRIzol reagent (15596026CN, Thermo), and quantified using NanoDrop 2000 and Agient2100/LabChip GX.

The total RNA was reversed by TransScript® Uni All-in-One First-Strand cDNA (TRANS, AU341) in a 20μL reaction system. The reversal transcription program was 25°C for 5min, 42°C for 30min, and 85°C for 5s. Primers were designed and synthesized by Sangon (Shanghai, China; Table 1). Amplification was performed on an ABI 7900 system (Foster City, CA, USA) and calculated using the $2^{-\Delta\Delta Ct}$ method With GAPDH as the reference gene. All experiments were tripled.

Western Blotting

Nrf2, HO-1, NQO1, Bax, Bcl-2, Caspase-3, Reg3g and GAPDH protein expression were assessed via Western blotting. The protein concentrations were measured using Pierce™ BCA Protein Assay Kit (no. 23227; Thermo Scientific, USA).

SDS-PAGE was performed under 120V. The PVDF membrane was washed with Tween-20: TBS = 1:1,000 for 5 minutes and blocked for 2h with 5% skimmed milk powder at room temperature. Primary antibodies Nrf2 (BF8017, Affinity), HO-1 (BF8020, Affinity), NQO1 (DF6427, Affinity), Bax (50599-2-Ig, Wuhan Sanying, China), Bcl-2 (AF6139, Wuhan Sanying), Caspase-3 (19677-1-AP, Wuhan Sanying), Reg3g (DF6869, Affinity) and GAPDH (60004-1-2-1g, Wuhan Sanying) were applied overnight. Subsequently, incubated with the secondary antibody of HRP-labeled goat anti-rabbit/mouse IgG. The PVDF membrane was then incubated with electrogenerated chemiluminescence (ECL) solution (ECL808-25, Biomiga, San Diego, CA, USA) and exposed. Band net density was calculated using Image J, with GAPDH as an internal reference band. All the experiments were repeated three times.

RNA Sequencing Data Generation, Processing, and Alignment

NC, T2DM, OLTI, and MET specimens underwent transcriptomic assessment, utilizing total RNA from pancreatic tissue. The Truseq Stranded mRNA LT Sample Prep kit was employed followed by a library constructed using the TruSeq Stranded mRNA Library Prep Kit (Illumina, San Diego, CA, United States). Sequencing used the Illumina NovaSeq6000 sequencing system with paired-end 150bp according to the manufacturer's protocols (Illumina, San Diego, CA, United States). Raw data was qualified by fastqc, aligning to the mice reference genome of NCBIM37. FDR (False Discovery Rate) was employed in this experiment to screen for differentially expressed genes.

DEGs Identification and KEGG Analysis

DEGs were identified using the thresholds of |log fold change (FC)| >1.5 and $P<0.05$. KEGG analysis was carried out using an online tool (https://www.omicshare.com/).

Table 1 The List of Primers

Genes	Forward Primer (5′-3′)	Reverse Primer (5′-3′)
Nrf2	GCGACAGAAGGACTATGAGCTGG	CCACTGGTGTCTGTCTGGATGTG
HO-1	CCCCACCAAGTTCAAACAGCTCT	ATCACCTGCAGCTCCTCAAACAG
NQO1	GAAGAGCCCTGATTGTACTGGCC	TCTTCGAGTCCTTCAGCTCACCT
Bax	GTTTCATCCAGGATCGAGCAGGG	GTGTCCACGTCAGCAATCATCCT
Bcl-2	ACTCTTCAGGGATGGGGTGAACT	TACTCAGTCATCCACAGGGCGAT
Caspase-3	TCACTCGCGTTAACAGGAAGGTG	TGAGCATGGACACAATACACGGG
Reg3g	AGTTGCCAAGAAAGATGCCCCAT	GATGTCCTGAGGGCCTCTTTTGG
GAPDH	GCCCAGAACATCATCCCTGCAT	GCCTGCTTCACCACCTTCTTGA

Note: GAPDH was used as the reference gene for Nrf2, HO-1, NQO1, Bax, Bcl-2, Caspase-3, and Reg3g.

Statistical Analysis

GraphPad Prism 9 (San Diego, CA, USA) was employed for statistical analysis and images. Unpaired Student's *t*-test and one-way ANOVA analyses were performed depending on the groups. Data are exhibited as mean ± standard deviation (SD). $P<0.05$ was considered a significant difference.

Results

Transcriptome Analysis

Sequencing Data Calculation

Post quality control, a total of 81.41 GB of clean data was obtained with the Q30 > 93.86% (Table 2), which is high-quality enough for the following analysis. Of all the samples, the least clean bases are 5879995800bp, providing ample scope for in-depth research. The GC content ranged from 49.74% to 50.52%.

DEGs Identification

With the thresholds of |logFC| >1.5 and $P<0.05$, the DEGs in five groups were identified and listed in Table 3. Significant downregulation was observed in the comparison groups with NC; T2DM_vs_NC had 370 (85 upregulated and 285 downregulated), MET_vs_NC had 349 (64 upregulated and 285 downregulated), and OLTI_vs_NC had 260 (94 upregulated and 166 downregulated) DEGs. A total of 50 DEGs were identified across all three groups (Figure S1A).

Table 2 The Sequencing Data Calculation

Samples	Clean Reads	Clean Bases (bp)	GC Content (%)	%≥Q30
NC1	21,566,140	6,469,842,000	50.05%	95.34%
NC2	21,227,477	6,368,243,100	50.06%	94.90%
NC3	22,529,660	6,758,898,000	49.99%	94.95%
T2DM1	25,721,927	7,716,578,100	50.27%	94.60%
T2DM2	21,223,731	6,367,119,300	50.52%	94.83%
T2DM3	26,325,423	7,897,626,900	49.98%	95.04%
MET1	25,503,711	7,651,113,300	49.74%	94.89%
MET2	19,599,986	5,879,995,800	50.10%	94.81%
MET3	23,035,173	6,910,551,900	49.96%	94.97%
OLTI1	22,452,487	6,735,746,100	49.94%	93.86%
OLTI2	22,018,704	6,605,611,200	49.95%	94.74%
OLTI3	20,161,063	6,048,318,900	49.87%	95.07%

Table 3 The Number of DEGs in Groups

Groups	All DEGs	Up-regulated	Down-regulated
T2DM_vs_NC	370	85	285
MET_vs_NC	349	64	285
OLTI_vs_NC	260	94	166
MET_vs_T2DM	274	135	139
OLTI_vs_T2DM	256	76	180

Npas2, Ccm21, Acap1, Gulo, Ciart, and C8b were significantly dysregulated in the T2DM group compared with the NC group (Table 4). Lck, Fcmr, and Csf2rb2 were significantly downregulated, while Slc22a27, Krt25, and Oas2 were significantly upregulated in the MET group compared with the NC group. Susd1, Kif23, Zkscan4, Syt5, Trp73, and Oas2 were significantly dysregulated in the OLTI group compared with the NC group.

Following treatments with metformin and oltipraz, DEGs were screened when compared with T2DM. In the MET_vs_T2DM group, 274 DEGs were identified, including 135 upregulated and 139 downregulated, and 256 DEGs (76 upregulated and 180 downregulated) in OLTI_vs_T2DM. A total of 79 DEGs were shared between MET_vs_T2DM and OLTI_vs_T2DM (Figure S1B). As listed in Table 4, Ccm2l, Hcn1, Npas2, Apoc1, Dph5, and Igkv3-2 were significantly dysregulated in MET_vs_T2DM, while Clip3, Npas2, Arg1, S1pr1, Dph5, and Igkv4-59 were significantly dysregulated in OLTI_vs_T2DM. Notably, the top downregulated Npsa2 and upregulated Dph5 were identified in both MET_vs_T2DM and OLTI_vs_T2DM. Moreover, Reg3g exhibits reduced expression in T2DM_vs_NC, and elevated expression in OLTI_vs_T2DM, yet remains unchanged in MET_vs_T2DM. These findings indicate that Reg3g may serve as a potential therapeutic target for OLTI (data not shown in the table).

Table 4 The Top ten Up-Regulated and Down-Regulated DEGs Were in Five Groups

T2DM_vs_NC		MET_vs_NC		OLTI_vs_NC		MET_vs_T2DM		OLTI_vs_T2DM	
DEGs	LogFC	DEGs	LogFC	DEGs	LogFC	DEGs	LogFC	DEGs	LogFC
Npas2	−7.27	Lck	−21.81	Susd1	−5.61	Ccm2l	−6.13	Clip3	−6.61
Ccm2l	−6.10	Fcmr	−7.21	Kif23	−5.48	Hcn1	−5.79	Npas2	−6.53
Acap1	−6.06	Csf2rb2	−6.88	Zkscan4	−5.42	Npas2	−5.74	Arg1	−5.98
Clip3	−5.98	Ighv7-3	−6.78	Prdm5	−5.39	Prkn	−5.69	Trpc1	−5.93
Rasgrp1	−5.94	Il21r	−6.75	Aim2	−5.22	Sh3tc2	−5.56	Nxpe2	−5.92
Vps37d	−5.62	H2-Ob	−6.68	Pole	−5.20	Cenpt	−5.46	Slc18a2	−5.83
Pole	−5.53	Fmr1nb	−6.64	Tmod2	−5.20	Kcnab2	−5.18	Mrln	−5.75
Abcg3	−5.49	Arhgap4	−6.64	Dnah11	−5.18	Arhgef38	−5.18	Jph2	−5.71
Gjd2	−5.44	Ms4a1	−6.63	Asb2	−5.13	Adamts14	−5.08	Trp73	−5.66
Aff3	−5.41	Slc36a2	−6.37	Aff3	−5.07	Zfp558	−5.08	Ccm2l	−5.56
Snai1	4.14	Ciart	2.94	Adamts6	4.74	Chrm2	5.08	Pde7b	4.79
Sgtb	4.34	Pgm5	3.27	C8b	4.81	Cdca7l	5.25	Srl	4.79
Oas2	4.67	Ncald	3.64	Pck1	4.88	Mx2	5.26	Lpxn	4.98
Prr3	4.79	Hpgds	4.01	Grin1	5.00	Gsto2	5.28	Chrm2	4.99
Ribc1	4.88	C8b	4.04	Snai1	5.07	Pole2	5.45	Mx2	5.17
Hpgds	4.90	Lrrc3	4.41	Otud7a	5.16	CRYBG3	5.57	Susd1	5.61
Crybg2	4.95	Fabp3	4.54	Prr3	5.27	Igkv8-24	5.61	Slc29a2	6.35
Gulo	5.02	Slc22a27	4.64	Syt5	5.32	Apoc1	5.92	S1pr1	6.38
Ciart	5.04	Krt25	5.33	Trp73	5.55	Dph5	6.29	Dph5	6.58
C8b	5.44	Oas2	5.53	Oas2	5.58	Igkv3-2	6.30	Igkv4-59	6.69

Abbreviations: DEGs, differentially expressed genes. FC, fold changes.

KEGG Analysis

KEGG analysis was performed on DEGs in five groups, with the top 25 KEGG terms depicted in Figure 1. In the T2DM_vs_NC group, DEGs predominantly implicated circadian rhythm, phenylalanine metabolism, Notch signaling

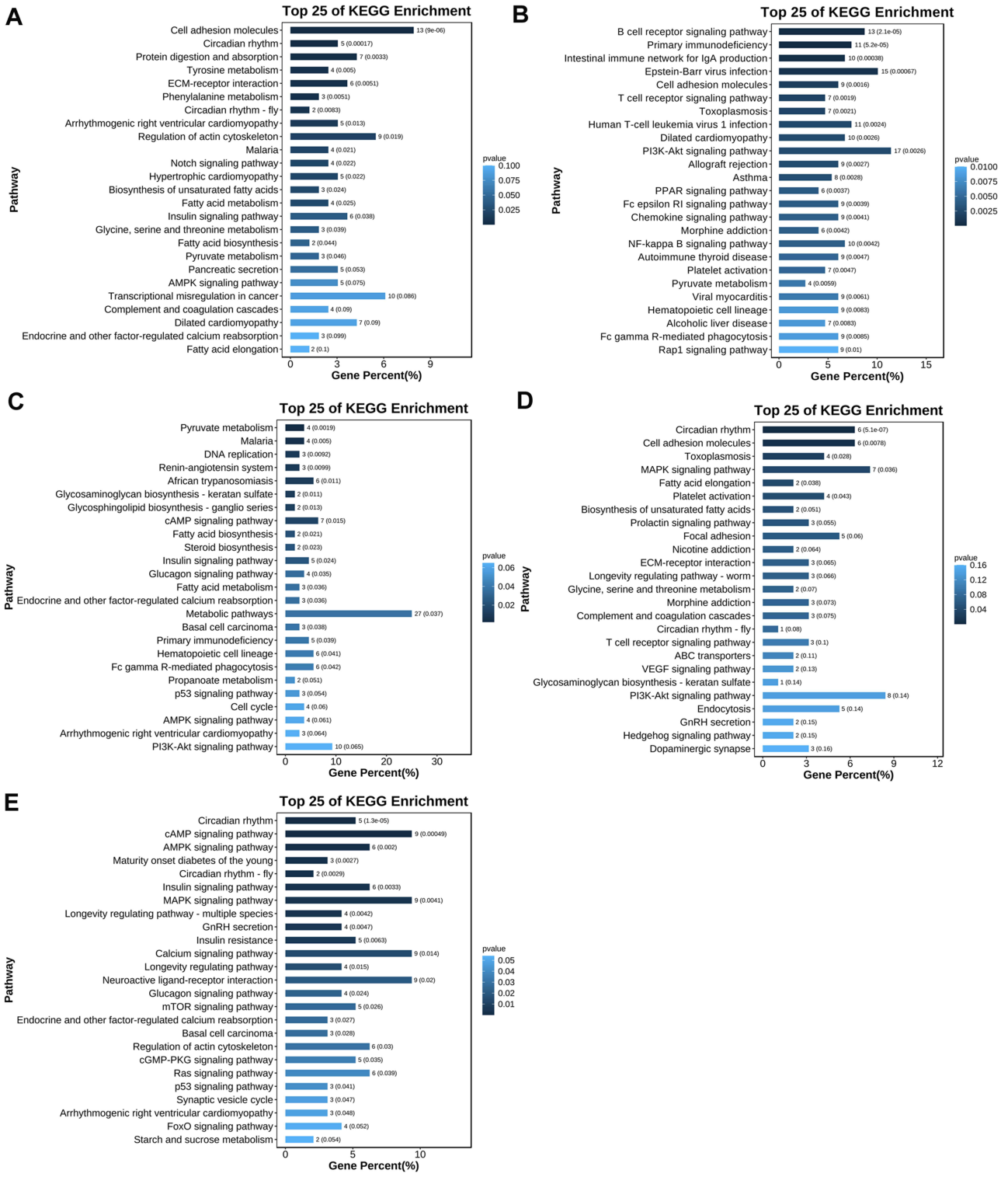

Figure 1 KEGG analysis of the T2DM_vs_NC(**A**), MET_vs_NC(**B**), OLTI_vs_NC(**C**), MET_vs_T2DM(**D**), and OLTI_vs_T2DM(**E**) groups. The top 25 enriched KEGG pathways were exhibited.

pathway, insulin signaling pathway, fatty acid biosynthesis, and pyruvate metabolism (Figure 1A). In the MET_vs_NC group, the B cell receptor signaling pathway, PI3K-Akt signaling pathway, PPAR signaling pathway, cAMP signaling pathway, and pyruvate metabolism pathway were significantly enriched (Figure 1B). In the OLTI_vs_NC group, pyruvate metabolism, cAMP signaling pathway, fatty acid biosynthesis, glucagon signaling pathway, and insulin signaling pathway were predominant (Figure 1C). In the MET_vs_T2DM group, circadian rhythm, cell adhesion molecules, toxoplasmosis, MAPK signaling pathway, fatty acid elongation, and platelet activation were enriched (Figure 1D). Lastly, in the OLTI_vs_T2DM group, circadian rhythm, cAMP signaling pathway, AMPK signaling pathway, circadian rhythm-fly pathway, insulin signaling pathway, and MAPK signaling pathway were enriched (Figure 1E). These findings suggest that glucose/fatty acid-related metabolism is essential for T2DM and is involved in MET and OLTI treatments, potentially providing insights into the molecular mechanism of T2DM therapeutics.

OLTI Reduces FBG and Relieves Body Weight Decrease Caused by T2DM

FBG was monitored throughout the whole experiment. Compared with the FBG value in the NC group (5.26±0.24mmol/L), it was significantly elevated in the T2DM group (17.56±0.38mmol/L) after being treated with STZ (P<0.001, Figure 2A). However, compared to the T2DM group (16.6±0.64mmol/L), the FBG in OLTI (12.83±1.67mmol/L) and MET (10.28±2.45mmol/L) groups were dramatically reduced after five days treatments (at 121 days) (P<0.01, P<0.001, Figure 2A). Notably, MET exhibited superior FBG reduction compared to OLTI at this time point (P<0.05). Ten days after treatments (at 126 days), the FBG in MET and OLTI became comparable. These results demonstrated that MET and

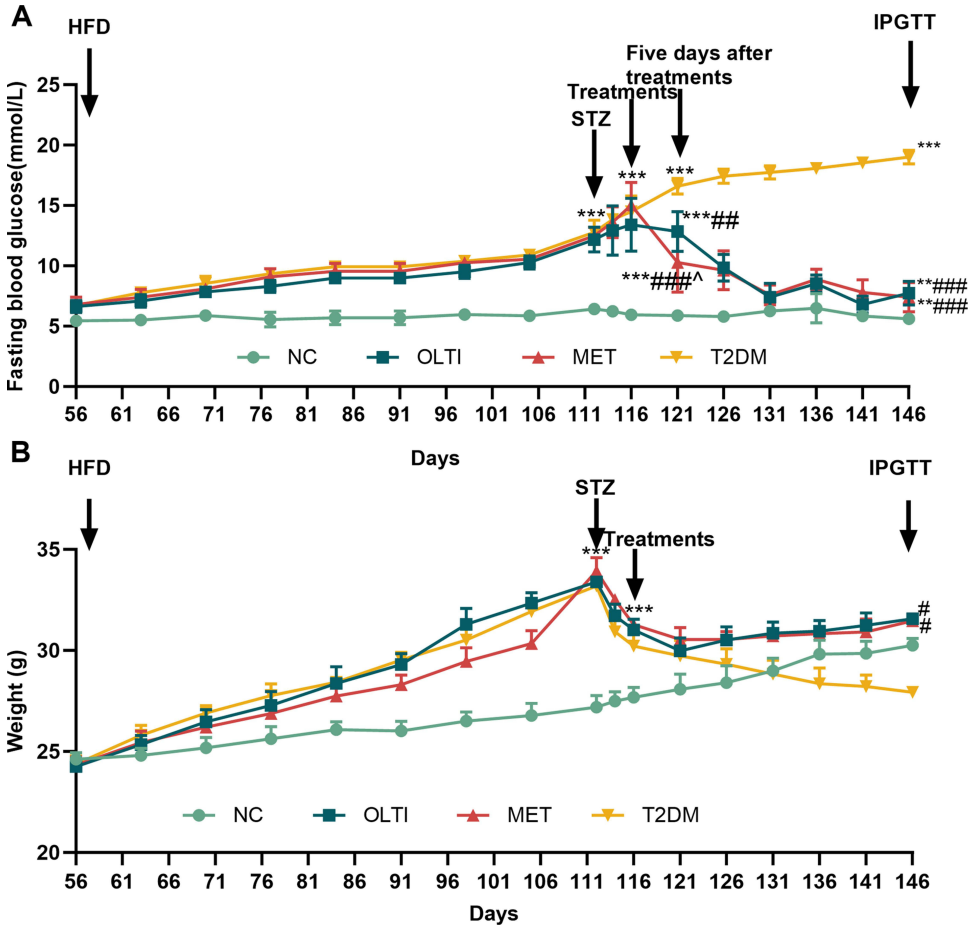

Figure 2 The effects of MET and OLTI on fasting blood glucose (**A**) and body weight (**B**). At 56 days, the animals were fed with a high-fat diet for eight weeks, then given STZ injections at 112 days to create the T2DM models. At 116 days, the T2DM models were treated with MET or OLTI. At 146 days, the IPGTT experiments were conducted. STZ means the time for STZ injection to build the T2DM model. Treatments mean the duration of MET and OLTI applications. IPGTT means at the experiment end for the intraperitoneal glucose tolerance test. **P<0.01 vs NC; ***P<0.001 vs NC. #P<0.05 vs T2DM; ##P<0.01 vs T2DM; ###P<0.001 vs T2DM. ^ P<0.05 vs MET.

OLTI exhibit similar long-term effects, yet MET has a superior immediate impact. As obverted from Figure 2A, the role of MET and OLTI in reducing FBG persists for over 30 days (from 116 days to 146 days).

High-fat diet progressively elevates mice's body weight. At 111 days (STZ point), the weight was significantly higher in the T2DM, MET, and OLTI groups compared to the NC group ($P<0.001$, Figure 2B). After treatments, the body weight in MET and OLTI groups gradually declined and stabilized, while it remained declined in the T2DM group, and subsequently increased in the NC group. There was no significant difference in body weight change between MET and OLTI. Therefore, OLTI exhibits a similar function to MET in reducing blood glucose and stabilizing body weight.

OLTI Reduces Blood Glucose and Insulin Resistance, and Decreases Blood Lipid Metabolism

As confirmed by IPGTT, glucose levels initially increased and then decreased in four groups (Figure 3A), reflecting glucose absorption and metabolism. For MET and OLTI groups, the peak occurred at 30 minutes, declining subsequently. The T2DM group experienced a peak at 60 minutes, indicating a delay compared with the MET and OLTI groups. The T2DM group exhibited the highest blood glucose level, followed by MET and OLTI treatment groups ($P<0.001$). Compared to the NC group, the IPGTT AUC was significantly increased in the T2DM, MET, and OLTI groups ($P<0.001$, Figure 3B). Following MET and OLTI treatment, the IPGTT AUC was significantly decreased ($P<0.001$). No significant difference was observed between MET and OLTI.

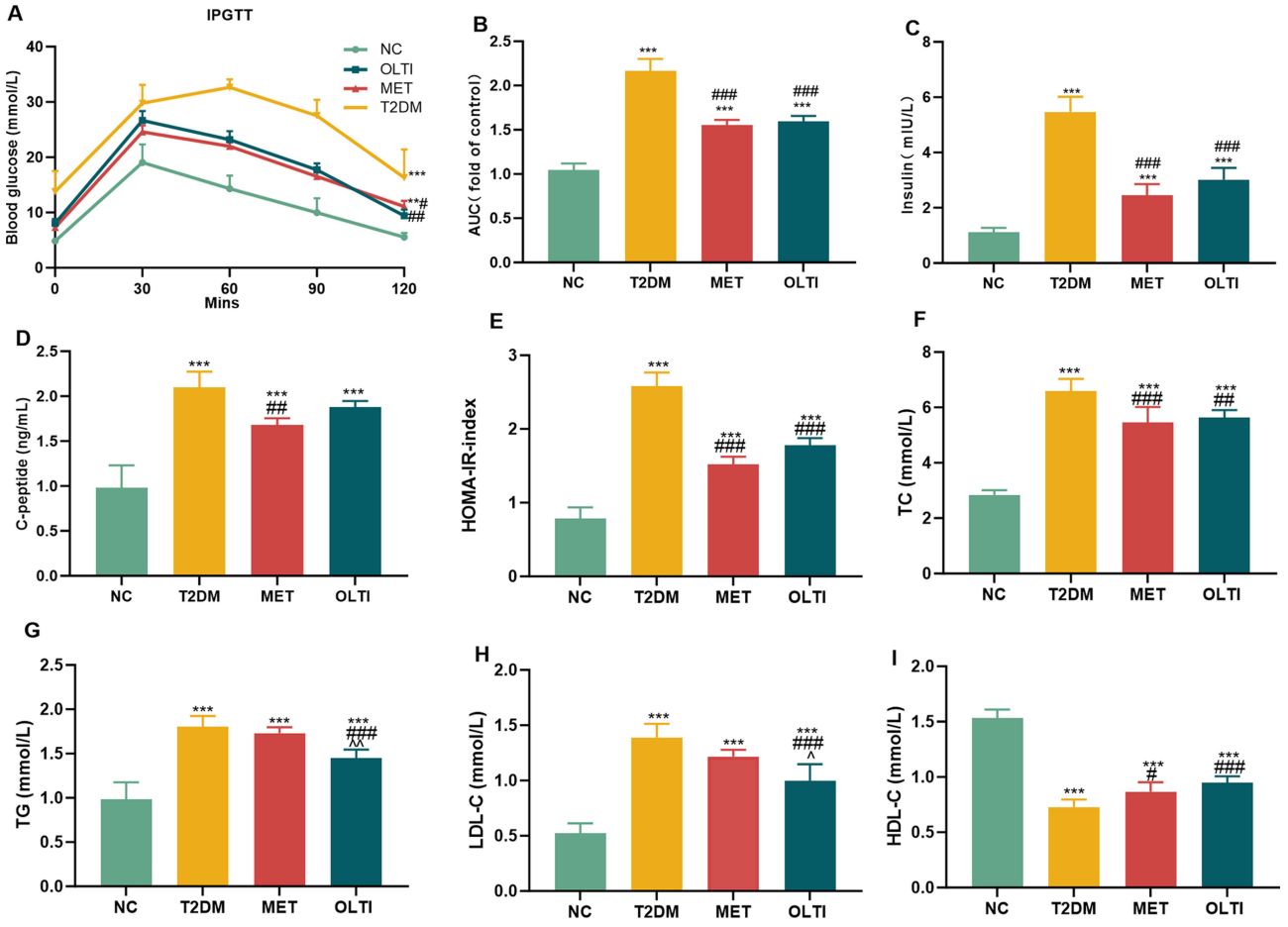

Figure 3 OLTI reduces blood glucose, insulin, C-peptide, HOMA-IR, and blood lipids. (**A**) The blood glucose levels were tested via IPGTT analysis. (**B**) The AUC of IPGTT was calculated in four groups. (**C–E**) The levels of insulin, C-peptide, and HOMA-IR index were measured in four groups. (**F–I**) The levels of blood lipids, including TC, TG, LDL-C, and HDL-C were measured in four groups. ***P*<0.01 vs NC; ****P*<0.001 vs NC. #*P*<0.05 vs T2DM; ##*P*<0.01 vs T2DM; ###*P*<0.001 vs T2DM. ^ *P*<0.05 vs MET, ^^ *P*<0.01 vs MET.

https://doi.org/10.2147/DDDT.S485729 DovePress

As detected in Figure 1C, the DEGs are primarily involved in fatty acid biosynthesis, glucagon signaling pathway, and insulin signaling pathway. Therefore, we examined insulin, glucose, and blood lipid levels in four groups. C-peptide is a crucial indicator of pancreatic function. Results showed that MET significantly reduced insulin, C-peptide, and HOMA-IR in T2DM models ($P<0.01$, $P<0.001$, Figure 3C–E). Conversely, OLTI significantly decreased insulin ($P<0.001$) and HOMA-IR ($P<0.001$) but not C-peptide ($P>0.05$) when compared to T2DM animals. The results indicated that OLTI-treated mice showed slightly higher insulin resistance than MET-treated mice.

TC, TG, HDL-C, and LDL-C levels were assessed in all groups. Compared to the T2DM group, MET and OLTI significantly reduced these levels, with minor differences ($P<0.01$, $P<0.001$, Figure 3F–I). Specifically, OLTI demonstrated superior effects on TG and LDL-C reduction, similar effects on TC reduction, and poorer effects on HDL-C reduction than MET. Collectively, OLTI demonstrated efficacy in reducing blood glucose, insulin resistance, and blood lipid metabolism.

OLTI Reduces Inflammation and Oxidative Stress, Relieves Pancreatic and Liver Tissue Injury, and Promotes Pancreatic β-Cell Secretion

Inflammation-related signaling pathways including cAMP, AMPK, and MAPK were enriched by DEGs in the OLTI_vs_T2DM group. Given the association of inflammation with oxidation stress, we detected the inflammatory factors and oxidative stress indexes in four groups.

ELISA assays quantified TNF-α, IL-1β, and IL-6 levels in four groups (Figure 4A–C). Significant differences were observed for TNF-α, IL-1β, and IL-6 between T2DM and NC, showing heightened inflammation factors in T2DM mice. These factors were significantly reduced in the OLTI group compared to T2DM. OLTI and MET exhibited comparable effects in reducing TNF-α, IL-1β, and IL-6 levels, demonstrating their anti-inflammatory functions in T2DM models.

To evaluate the role of OLTI in oxidation stress, the indexes of GSH-Px activity, SOD, ROS, and MDA were assessed. As shown in Figure 4D–G, OLTI showed superior effects in enhancing GSH-Px activity and SOD, decreasing MDA and ROS compared to MET ($P<0.05$, $P<0.001$). This suggests that OLTI can effectively improve the level of antioxidize, reduce MDA content, improve antioxidant capabilities, and clear free radicals.

HE staining revealed significant differences in pancreatic and liver tissues among the four groups and the ratio of islet area to the pancreatic area was elevated (Figure 4H and L). In the NC group, the pancreatic tissue appeared normal, with clear islet cell outlines, abundant β-cells, and no obvious loose edema, necrosis, and inflammation cell infiltrate. However, the T2DM group displayed abnormal structures with distorted pancreatic structures, β-cell necrosis, and reduced venular epithelial cell enzymes. This anomaly may be attributed to insulin resistance in T2DM mice, leading to dysfunction and lesions. Compared to the T2DM group, tissues in OLTI and MET groups showed significantly reduced pathological severity, indicating a protective effect of OLTI and MET on pancreatic β-cells in T2DM mice, potentially linked to improved insulin resistance.

Therefore, the insulin immunofluorescence analysis in four groups was assessed (Figure 4I and M). In the NC group, the pancreas was intact with abundant insulin-positive particles, indicating normal β-cell function. In contrast, the T2DM group had significantly reduced β-cells, which increased following treatment with MET and OLTI. These findings suggest that OLTI and MET can effectively alleviate T2DM-induced pancreatic β-cell damage.

The role of OLTI on the pathological structure of liver tissues was assessed by HE staining (Figure 4J and K). In the NC group, the liver tissue was intact with uniform liver cells, non-fat degeneration, and no obvious inflammatory cell infiltration. The T2DM group exhibited abnormal structure with loose liver cell structure, obvious edema, abundant fat degeneration, and some inflammatory cell infiltration. OLTI and MET groups showed improved overall structure compared to the T2DM group, with no significant blood vessel expansion and obvious inflammatory cell infiltration. Additionally, OLTI alleviated fat degeneration compared to the MET group, showing improved blood lipids in T2DM models treated with OLTI.

OLTI Showed an Anti-Oxidation Stress and Anti-Apoptosis Function in T2DM

We also examined the expression of Reg3g, Nrf2/HO-1 signaling pathway, and cell apoptosis-related genes in four groups. Our findings indicate that the expression of Nrf2, HO-1, and NQO1 were significantly reduced in T2DM, yet

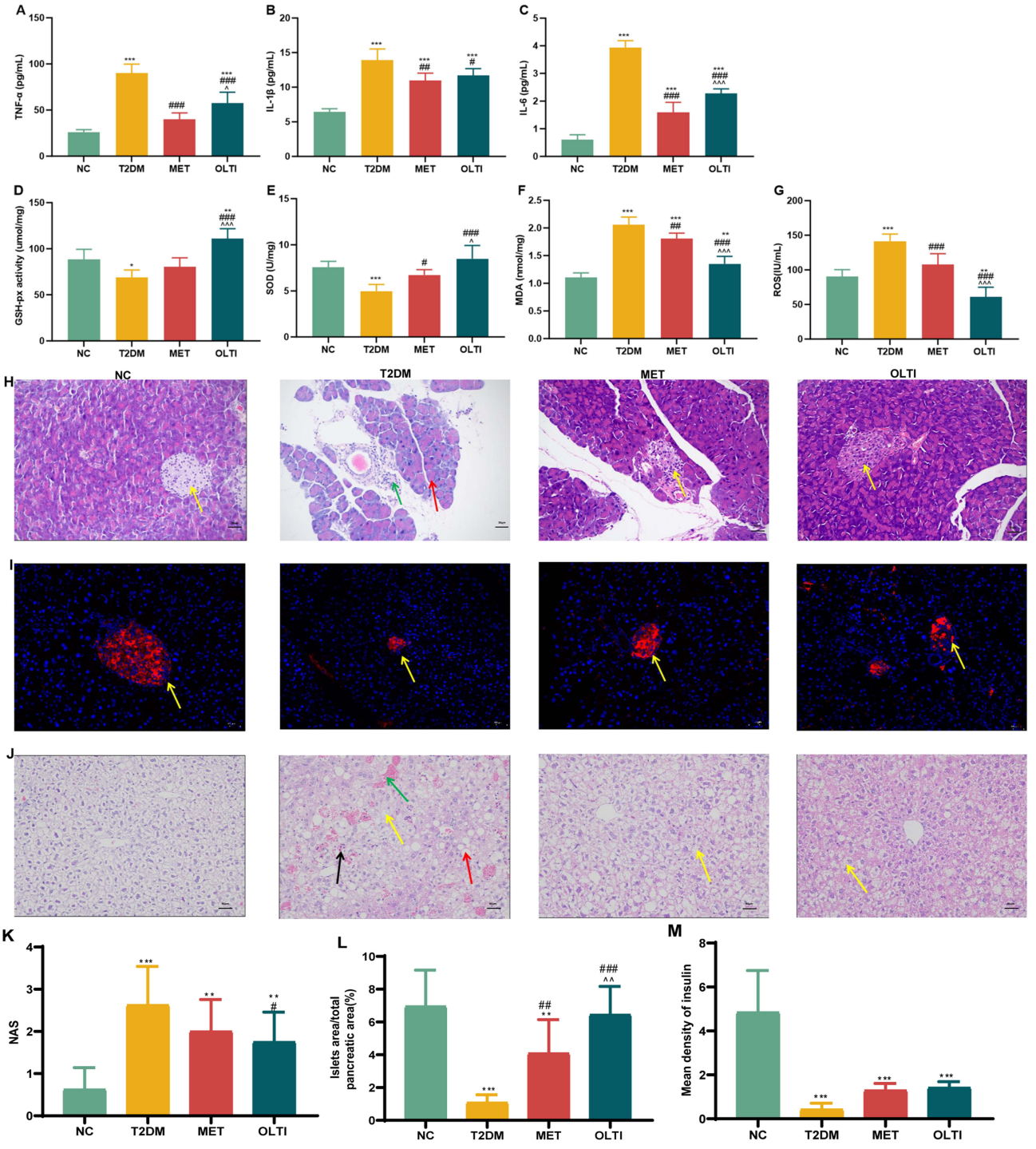

Figure 4 OLTI reduces inflammation and oxidation stress, relieves pancreas and liver tissue damage, and promotes pancreatic β-cells insulin secretion. (**A–C**) listed the levels of TNF-α, IL-1β, and IL-6 levels in four groups. (**D–G**) showed the GSH-Px activity, SOD, MDA, and ROS, respectively. (**H** and **L**) HE staining was performed on pancreatic tissues in four groups and islet area quantification was performed based on HE staining. Note: Yellow arrow: pancreas; green arrows: pancreas cell necrosis; red arrow: glands of epithelial cells. (**I** and **M**) Immunofluorescence detection of insulin protein levels in pancreas tissues. Note: Yellow arrow: pancreas. (**J** and **K**) HE staining was performed on liver tissues in four groups and NAFLD Activity Score (NAS). Note: Yellow arrow: hepatocyte edema; Red arrow: fat degeneration; Black arrow: inflammation cells; Green arrow: red cell. **P*<0.05 vs NC, ***P*<0.01 vs NC; ****P*<0.001 vs NC. #*P*<0.05 vs T2DM; ##*P*<0.01 vs T2DM; ###*P*<0.001 vs T2DM. ^*P*<0.05 vs MET, ^^*P*<0.01 vs MET, ^^^ *P*<0.001 vs MET.

increased upon treatment with MET and OLTI (*P*<0.01, *P*<0.001; Figure 5A–C and H–K). Notably, OLTI yields a superior effect on the Nrf2/HO-1 signaling pathway compared to MET (P<0.001), demonstrating greater anti-oxidation potential. The expression of Bax, Bcl-2, and Caspase-3, key cell apoptosis genes, were dysregulated in four

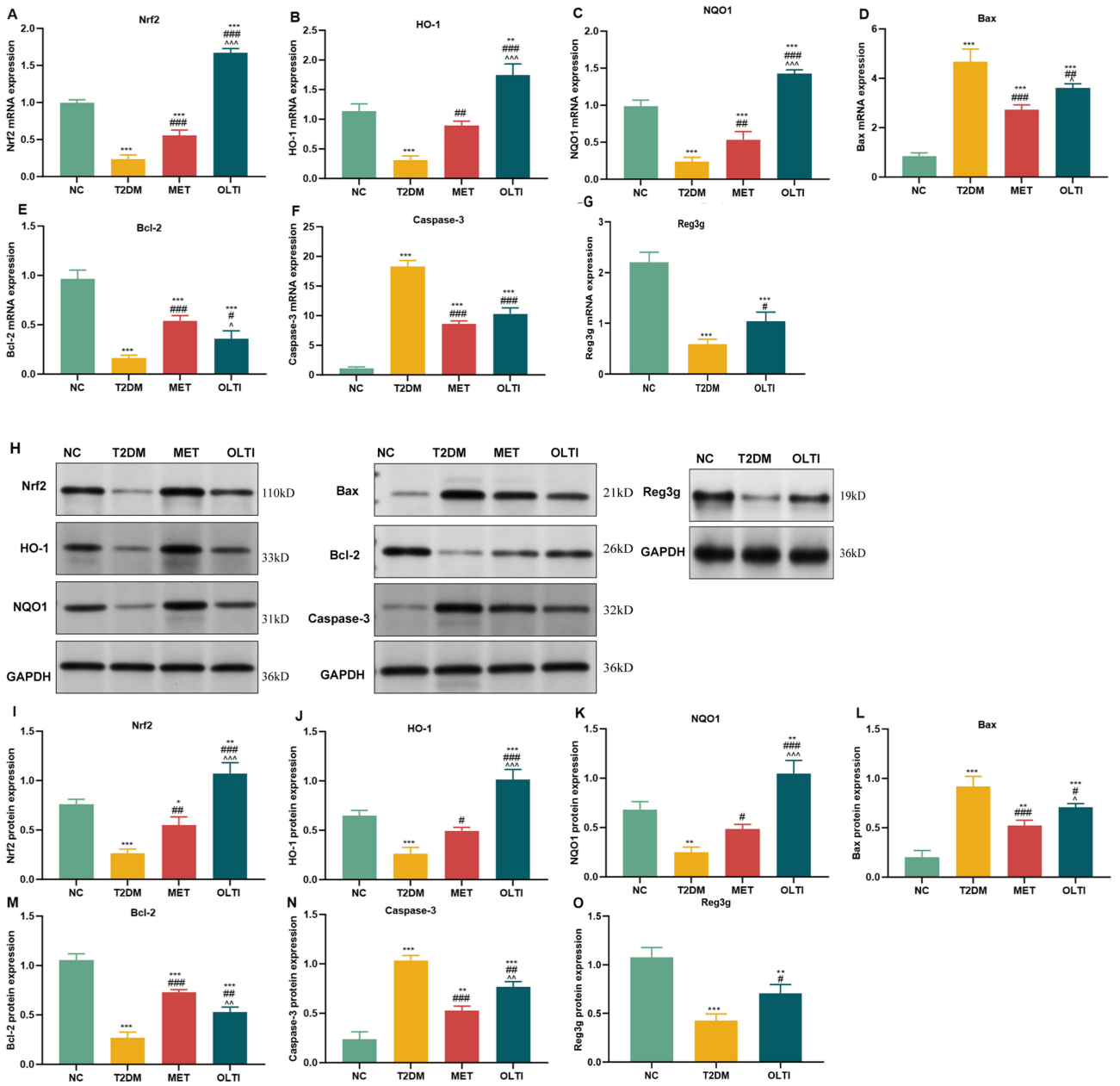

Figure 5 OLTI showed an anti-oxidation stress and anti-apoptosis function in T2DM. (**A–G**) the expression of Nrf2, HO-1, NQO1, Bax, Bcl-2, Caspase-3, and Reg3g in mRNA level. (**H–O**) the expression of Nrf2, HO-1, NQO1, Bax, Bcl-2, Caspase-3, and Reg3g in protein level. **P*<0.05 vs NC, ***P*<0.01 vs NC; ****P*<0.001 vs NC. #*P*<0.05 vs T2DM; ##*P*<0.01 vs T2DM; ###*P*<0.001 vs T2DM. ^ *P*<0.05 vs MET, ^^*P*<0.01 vs MET, ^^^ *P*<0.001 vs MET.

groups, with Bax and Caspase-3 highly expressed in T2DM, and then reversed by MET and OLTI treatments; Bcl-2 is lowly expressed in T2DM but enhanced by MET and OLTI treatments (*P*<0.01, *P*<0.001; Figure 5D–F and L–N). These results demonstrated that MET and OLTI alleviate T2DM-induced cell apoptosis. Specifically, OLTI exhibits a weaker anti-apoptosis function than the MET group as evidenced by the significant increase in Bax expression and decrease in Bcl-2 expression compared to the MET group. Moreover, the expression of Reg3g is significantly increased in the OLTI group compared to the T2DM group (*P*<0.05, Figure 5G, H, and O), indicating a pro-proliferation and anti-apoptosis role for OLTI. In conclusion, OLTI exhibits potent anti-oxidation stress and anti-apoptosis functions in T2DM.

Discussion

Oltipraz is clinically employed in cancer, liver fibrosis, and cirrhosis. However, the role of OLTI in regulating glucose and lipid metabolism, inflammation, oxidation stress, and insulin resistance in T2DM remains unclear. This study revealed the following: (1) DEGs and pathways are altered in MET and OLTI vs T2DM mice. (2) OLTI reduces fasting blood glucose and relieves body weight loss in T2DM. (3) OLTI reduces blood glucose, insulin resistance, and blood lipid metabolism. (4) OLTI reduces inflammation and oxidation stress, alleviates pancreas and liver tissue damage, and promotes pancreatic β-cell insulin secretion. (5) OLTI exhibits anti-oxidation stress and anti-apoptosis functions in T2DM.

In this study, Reg3g was dysregulated in OLTI_vs_T2DM, but not in MET_vs_T2DM. Reg3g, a multifunctional protein, suppresses epithelial inflammation and bacterial colonization, providing protective effects on colitis, diabetic wound healing, and alcohol-induced fatty liver disease.[27,28] As revealed, the pharmacological application of Reg3g improves glucose tolerance in DIO mice.[29] As demonstrated, the gut peptide Reg3g links the small intestine microbiome to the regulation of energy balance, glucose levels, and gut function.[29] Reg3g is also one susceptibility gene related to T2DM skeletal muscle.[30] In addition, previous studies have shown that Reg3g can activate the JAK2/STAT3 pathway to promote islet cell proliferation, improving DM symptoms in NOD mice.[10] In the iron excess mice model, increased Reg3g expression in the pancreas improves excessive iron-induced β-cell dysfunction and insulin secretion.[31] Upon increased Reg3g levels, reactive oxygen species (ROS) and inflammation factors were curtailed. Additionally, its scavenging properties exhibit antioxidant effects, mitigating pancreatic β cell oxidative damage.[32,33] These studies suggest Reg3g protects damaged cells, especially pancreatic β cells. These findings indicate that Reg3g could be an important target for OLTI treatment of T2DM.

Significantly enriched signaling pathways in the OLTI_vs_T2DM group include the cAMP, AMPK, insulin, and MAPK. At the cellular level, AMPK supports energy and redox homeostasis, including mitochondrial biogenesis, autophagy, and glucose and lipid metabolism. Thus, understanding these pathways is crucial for developing metabolic disorder treatments. Mounting evidence suggests a link between cAMP and AMPK signaling. cAMP signaling is activated during physiological and metabolic stress due to the release of stress hormones, such as adrenaline and glucagon, leading to membrane-bound adenylyl cyclase activation and cellular cAMP elevation. Given the association of physiological stress with elevated energy consumption, cAMP signaling may promote AMPK activity. Besides the physiological role of the cAMP/AMPK axis, numerous reports have suggested its role in several pathologies, including inflammation, ischemia, diabetes, obesity, and aging. Furthermore, novel reports have provided more mechanistic insight into the regulation of the cAMP/AMPK axis.[34] Therefore, OLTI's effect on T2DM patients likely involves inflammation, glucose, and lipid metabolism. Therefore, we further verified the role of OLTI in glucose and lipid metabolism, inflammation, and oxidation stress.

The primary pathological feature of T2DM is chronic hyperglycemia, the patients of T2DM are always in a state of high blood glucose for a long time, which induces dysfunctional and damaged pancreatic β cells, and enhances insulin resistance,[35] ultimately leading to glycolic toxicity.[36] Our study demonstrated that OLTI can improve T2DM mice insulin sensitivity, insulin resistance, and glucose metabolism, thereby alleviating DM disease.

Abnormal glucose metabolism is always accompanied by lipid metabolism disorders.[37] Insulin resistance induces lipid metabolism aberrations, decreases peripheral tissue insulin sensitivity, and reduces glucose utilization rate, which accelerates fat decomposition and elevates free fatty acids, increasing TC, TG, and LDL levels.[38] Our current study revealed that OLTI had a greater effect on reducing blood lipids than MET, which is consistent with prior research.[39]

The liver is a primary recipient of insulin function, which regulates energy metabolism.[40] In our present study, mice exhibiting severe pathological damage in T2DM were relieved after the OLTI treatment, showing reduced inflammatory cell infiltration and improved structure. This finding suggested that OLTI may improve lipid metabolism by reducing TC, TG, and LDL levels, as well as ameliorating insulin resistance.

There is a strong link between hyperglycemia, hyperglycemic-induced oxidative stress, inflammation, and T2DM development.[41] In our present study, we evaluated the role of OLTI in reducing inflammation, oxidative stress, and pancreatic tissue cell apoptosis. Various reports have shown that chronic low-grade inflammation is linked to T2DM risk, and sub-clinical inflammation contributes to insulin resistance and metabolic syndrome features such as hyperglycemia. Oxidative stress stimulates inflammatory mediators production, and inflammation enhances reactive oxygen species production.[42] Addressing oxidative stress could alleviate the diabetes burden and improve patient outcomes. Our study found that OLTI attenuated

oxidative stress in T2DM animals, consistent with the previous studies.[43,44] Jiang et al[43] reported that OLTI prevents high-glucose-induced oxidative stress and cell apoptosis through the Nrf2/NQO1 signaling pathway. Notably, we found that OLTI showed superior anti-oxidation and weaker anti-apoptosis effects than MET, which has rarely been reported before.

Nrf2 is a key antioxidant molecule involved in cell protection. Under normal physiological conditions, Nrf2 exists in the cytoplasm bound to kelch-like ECH-associated protein 1 (KEAP1) and is degraded by protease through ubiquitination, showing an inhibited activity of Nrf2.[45] Oxidation stress triggers Nrf2 transfer to the nucleus, binding to the antioxidant response (ARS), and promoting ARS-regulated genes.[46,47] Nrf2 can also be activated by AMPK, to play an anti-oxidation function by initiating downstream antioxidant enzymes reactions, such as glutathione reductase (GR), glutathione hormone (GSH), GSH-Px, catalase (CAT), superoxide dismutase (SOD), HO-1, and quinone oxidoreductase 1 (NQO1).[48–51] Furthermore, enhancing the Nrf2 and HO-1 alleviates inflammation in acute pancreatitis mouse models.[52] The Nrf2/HO-1 pathway plays an important role in regulating T2DM oxidative stress reactions.

However, these are some limitations of our present study. First, the OLTI experiment on T2DM animals lasted 30 days, since type 2 diabetes is a chronic disease, this is an essential issue to address. Whether Oltipraz possesses the potential to sustain its beneficial effects over extended periods of therapy remains uncertain, warranting future studies on its safety and efficacy over time. Second, the detailed molecular mechanism by which Nrf2, HO-1, and Reg3g regulate oxidation and cell apoptosis requires further study.

Conclusion

In summary, we explored the role of OLTI in glucose and lipid metabolism, inflammation, oxidative stress, and apoptosis in T2DM mice models. We compared OLTI's functions with metformin. Through this study, the findings indicated that OLTI improves blood glucose and insulin resistance, decreases blood lipid metabolism, reduces inflammation and apoptosis, promotes anti-oxidative stress through the Nrf2/HO-1 signaling pathway, mitigates pancreatic and liver tissue injury, and enhances pancreatic β-cell insulin secretion, thus attenuating T2DM symptoms. Moreover, Reg3g preserves pancreatic beta cell function, potentially a crucial target for the treatment of T2DM with OLTI, vital in optimizing diabetes management. Simultaneously, due to the potential liver toxicity of high doses of Oltipraz in other contexts, further investigation into its long-term consequences is warranted. And Oltipraz could be incorporated into current T2DM therapeutic regimens, potentially enhancing efficacy when paired with existing medications such as metformin.

Data Sharing Statement

The raw RNA-seq data were submitted to NCBI (https://www.ncbi.nlm.nih.gov/) with the accession number PRJNA1108402.

Ethical Approval

Animal care and experimental procedures were performed according to the Guidelines for Animal Experimentation of Nanchang University, with approval from the Nanchang University Experimental Animal Ethics Committee.

Author Contributions

All authors made a significant contribution to the work reported, whether that is in the conception, study design, execution, acquisition of data, analysis and interpretation, or in all these areas; took part in drafting, revising or critically reviewing the article; gave final approval of the version to be published; have agreed on the journal to which the article has been submitted; and agree to be accountable for all aspects of the work.

Funding

This work was supported by the National Natural Science Foundation of China (82160162, 81760150) and the Project of the Second Affiliated Hospital of Nanchang University (2022efyA04).

Disclosure

No competing financial interests exist.

References

1. Prasad M, Chen EW, Toh S-A, Gascoigne NR. Autoimmune responses and inflammation in type 2 diabetes. *J Leukocyte Biol*. 2020;107(5):739–748. doi:10.1002/JLB.3MR0220-243R
2. Zheng Y, Ley SH, Hu FB. Global aetiology and epidemiology of type 2 diabetes mellitus and its complications. *Nat Rev Endocrinol*. 2018;14(2):88–98. doi:10.1038/nrendo.2017.151
3. Ng ML, Wadham C, Sukocheva OA. The role of sphingolipid signalling in diabetes-associated pathologies. *Int J Mol Med*. 2017;39(2):243–252. doi:10.3892/ijmm.2017.2855
4. Azarova I, Klyosova E, Polonikov A. The link between type 2 diabetes mellitus and the polymorphisms of glutathione-metabolizing genes suggests a new hypothesis explaining disease initiation and progression. *Life*. 2021;11(9):886. doi:10.3390/life11090886
5. Li H, Zhao K, Li Y. Gasdermin D influence mouse podocytes against high-glucose-induced inflammation and apoptosis via the C-Jun N-Terminal Kinase (JNK) pathway. *Med Sci Monit*. 2021;27:e928411. doi:10.12659/MSM.928411
6. Fang Y, Ma J, Lei P, et al. Konjac glucomannan: an emerging specialty medical food to aid in the treatment of type 2 diabetes mellitus. *Foods*. 2023;12(2):363. doi:10.3390/foods12020363
7. McIntyre TM, Hazen SL. Lipid oxidation and cardiovascular disease: introduction to a review series. *Circ Res*. 2010;107(10):1167–1169. doi:10.1161/CIRCRESAHA.110.224618
8. Zhang Y, Liu Y, Liu X, et al. Exercise and metformin intervention prevents lipotoxicity-induced hepatocyte apoptosis by alleviating oxidative and ER stress and activating the AMPK/Nrf2/HO-1 signaling pathway in db/db mice. *Oxid Med Cell Long*. 2022;2022:2297268.
9. Gerber PA, Rutter GA. The role of oxidative stress and hypoxia in pancreatic beta-cell dysfunction in diabetes mellitus. *Antioxid Redox Signal*. 2017;26(10):501–518. doi:10.1089/ars.2016.6755
10. Xia F, Cao H, Du J, Liu X, Liu Y, Xiang M. Reg3g overexpression promotes β cell regeneration and induces immune tolerance in nonobese-diabetic mouse model. *J Leukocyte Biol*. 2016;99(6):1131–1140. doi:10.1189/jlb.3A0815-371RRR
11. Li S, Zhou H, Xie M, et al. Regenerating islet-derived protein 3 gamma (Reg3g) ameliorates tacrolimus-induced pancreatic β-cell dysfunction in mice by restoring mitochondrial function. *Br J Pharmacol*. 2022;179(12):3078–3095. doi:10.1111/bph.15803
12. Butt SM. Management and treatment of type 2 diabetes. *Int J Comput Integr Manuf*. 2022;2(1).
13. Zhou YQ, Liu DQ, Chen SP, et al. PPARγ activation mitigates mechanical allodynia in paclitaxel-induced neuropathic pain via induction of Nrf2/HO-1 signaling pathway. *Biomed Pharmacother*. 2020;129:110356. doi:10.1016/j.biopha.2020.110356
14. Kim SG, Kim YM, Choi JY, et al. Oltipraz therapy in patients with liver fibrosis or cirrhosis: a randomized, double-blind, placebo-controlled phase II trial. *J Pharm Pharmacol*. 2011;63(5):627–635. doi:10.1111/j.2042-7158.2011.01259.x
15. Masubuchi Y, Mikami K. Efficacy of oltipraz in preventing acetaminophen-induced liver injury in mice. *Naunyn-Schmiedeberg's Arch Pharmacol*. 2024;397(2):923–930. doi:10.1007/s00210-023-02649-5
16. Nelson KC, Armstrong JS, Moriarty S, et al. Protection of retinal pigment epithelial cells from oxidative damage by oltipraz, a cancer chemopreventive agent. *Invest Ophthalmol Visual Sci*. 2002;43(11):3550–3554.
17. Rooney JP, Chorley B, Hiemstra S, et al. Mining a human transcriptome database for chemical modulators of NRF2. *PLoS One*. 2020;15(9):e0239367. doi:10.1371/journal.pone.0239367
18. de Haan JB. Nrf2 activators as attractive therapeutics for diabetic nephropathy. *Diabetes*. 2011;60(11):2683–2684. doi:10.2337/db11-1072
19. Malhotra JD, Kaufman RJ. Endoplasmic reticulum stress and oxidative stress: a vicious cycle or a double-edged sword? *Antioxid Redox Signal*. 2007;9(12):2277–2293. doi:10.1089/ars.2007.1782
20. Zhang X, Zhang Y, Zhou M, et al. DPHC from Alpinia officinarum ameliorates oxidative stress and insulin resistance via activation of Nrf2/ARE pathway in db/db mice and high glucose-treated HepG2 cells. *Front Pharmacol*. 2021;12:792977. doi:10.3389/fphar.2021.792977
21. Yagishita Y, Gatbonton-Schwager TN, McCallum ML, Kensler TW. Current landscape of NRF2 biomarkers in clinical trials. *Antioxidants*. 2020;9(8):716. doi:10.3390/antiox9080716
22. Merrell MD, Jackson JP, Augustine LM, et al. The Nrf2 activator oltipraz also activates the constitutive androstane receptor. *Drug Metab Dispos*. 2008;36(8):1716–1721. doi:10.1124/dmd.108.020867
23. Zhou Y-Q, Liu D-Q, Chen S-P, et al. Nrf2 activation ameliorates mechanical allodynia in paclitaxel-induced neuropathic pain. *Acta Pharmacol Sin*. 2020;41(8):1041–1048. doi:10.1038/s41401-020-0394-6
24. Apostolova N, Iannantuoni F, Gruevska A, Muntane J, Rocha M, Victor VM. Mechanisms of action of metformin in type 2 diabetes: effects on mitochondria and leukocyte-endothelium interactions. *Redox Biol*. 2020;34:101517. doi:10.1016/j.redox.2020.101517
25. Sun CC, Lai YN, Wang WH, et al. Metformin ameliorates gestational diabetes mellitus-induced endothelial dysfunction via downregulation of p65 and upregulation of Nrf2. *Front Pharmacol*. 2020;11:575390. doi:10.3389/fphar.2020.575390
26. Trovato FM, Catalano D, Musumeci G, Trovato GM. 4Ps medicine of the fatty liver: the research model of predictive, preventive, personalized and participatory medicine-recommendations for facing obesity, fatty liver and fibrosis epidemics. *EPMA J*. 2014;5(1):21. doi:10.1186/1878-5085-5-21
27. Darnaud M, Dos Santos A, Gonzalez P, et al. Enteric delivery of regenerating family member 3 alpha alters the intestinal microbiota and controls inflammation in mice with colitis. *Gastroenterology*. 2018;154(4):1009–1023.e14. doi:10.1053/j.gastro.2017.11.003
28. Greenhill C. REG3G—a potential link between the intestinal microbiome and host physiology. *Nat Rev Endocrinol*. 2023;19(1):5. doi:10.1038/s41574-022-00774-4
29. Shin JH, Bozadjieva-Kramer N, Shao Y, et al. The gut peptide Reg3g links the small intestine microbiome to the regulation of energy balance, glucose levels, and gut function. *Cell Metab*. 2022;34(11):1765–1778.e6. doi:10.1016/j.cmet.2022.09.024
30. Ke J, Hu X, Wang C, Zhang Y. Identification of the hub susceptibility genes and related common transcription factors in the skeletal muscle of type 2 diabetes mellitus. *BMC Endocr Disord*. 2022;22(1):276. doi:10.1186/s12902-022-01195-0
31. Backe MB, Moen IW, Ellervik C, Hansen JB, Mandrup-Poulsen T. Iron regulation of pancreatic beta-cell functions and oxidative stress. *Ann Rev Nutr*. 2016;36:241–273. doi:10.1146/annurev-nutr-071715-050939
32. Lei P, Chen H, Ma J, et al. Research progress on extraction technology and biomedical function of natural sugar substitutes. *Front Nutr*. 2022;9:952147. doi:10.3389/fnut.2022.952147
33. Xia T, Zhang B, Li S, et al. Vinegar extract ameliorates alcohol-induced liver damage associated with the modulation of gut microbiota in mice. *Food Funct*. 2020;11(4):2898–2909. doi:10.1039/c9fo03015h

34. Aslam M, Ladilov Y. Emerging role of cAMP/AMPK signaling. *Cells*. 2022;11(2):308. doi:10.3390/cells11020308
35. Marušić M, Paić M, Knobloch M, Liberati Pršo A-M. NAFLD, insulin resistance, and diabetes mellitus type 2. *Can J Gastroenterol Hepatol*. 2021;2021:1–9. doi:10.1155/2021/6613827
36. Kahn SE, Hull RL, Utzschneider KM. Mechanisms linking obesity to insulin resistance and type 2 diabetes. *Nature*. 2006;444(7121):840–846. doi:10.1038/nature05482
37. Chen Z, Zhao G, Zhang Y, Shen G, Xu Y, Xu N. Research on the correlation of diabetes mellitus complicated with osteoporosis with lipid metabolism, adipokines and inflammatory factors and its regression analysis. *Eur Rev Med Pharmacol Sci*. 2017;21(17):3900–3905.
38. Sarkar PD, Choudhury AB. Relationship of serum osteocalcin levels with blood glucose, insulin resistance and lipid profile in central Indian men with type 2 diabetes. *Arch Phys Biochem*. 2012;118(5):260–264. doi:10.3109/13813455.2012.715651
39. Yu Z, Shao W, Chiang Y, et al. Oltipraz upregulates the nuclear factor (erythroid-derived 2)-like 2 [corrected](NRF2) antioxidant system and prevents insulin resistance and obesity induced by a high-fat diet in C57BL/6J mice. *Diabetologia*. 2010;54(4):922–934. doi:10.1007/s00125-010-2001-8
40. Yan J, Wang C, Jin Y, et al. Catalpol ameliorates hepatic insulin resistance in type 2 diabetes through acting on AMPK/NOX4/PI3K/AKT pathway. *Pharmacol Res*. 2018;130:466–480. doi:10.1016/j.phrs.2017.12.026
41. Oguntibeju OO. Type 2 diabetes mellitus, oxidative stress and inflammation: examining the links. *Int J Physiol Pathophysiol Pharmacol*. 2019;11(3):45.
42. Caturano A, D'Angelo M, Mormone A, et al. Oxidative stress in type 2 diabetes: impacts from pathogenesis to lifestyle modifications. *Curr Issues Mol Biol*. 2023;45(8):6651–6666. doi:10.3390/cimb45080420
43. Jiang Z, Bian M, Wu J, Li D, Ding L, Zeng Q. Oltipraz prevents high glucose-induced oxidative stress and apoptosis in RSC96 cells through the Nrf2/NQO1 signalling pathway. *Biomed Res Int*. 2020;2020:1–8. doi:10.1155/2020/5939815
44. Tang Y, Guo M, Ma X-Y, Sun W-P, Hao M-H, Zhu H-Y. Oltipraz attenuates the progression of heart failure in rats through inhibiting oxidative stress and inflammatory response. *Eur Rev Med Pharmacol Sci*. 2018;22(24).
45. Silva-Palacios A, Ostolga-Chavarría M, Zazueta C, Königsberg M. Nrf2: molecular and epigenetic regulation during aging. *Ageing Res Rev*. 2018;47:31–40. doi:10.1016/j.arr.2018.06.003
46. Li B, Nasser M, Masood M, et al. Efficiency of traditional Chinese medicine targeting the Nrf2/HO-1 signaling pathway. *Biomed Pharmacother*. 2020;126:110074. doi:10.1016/j.biopha.2020.110074
47. Liu X-F, Zhou -D-D, Xie T, et al. The Nrf2 signaling in retinal ganglion cells under oxidative stress in ocular neurodegenerative diseases. *Int J Bio Sci*. 2018;14(9):1090. doi:10.7150/ijbs.25996
48. Huang BP, Lin CH, Chen HM, Lin JT, Cheng YF, Kao SH. AMPK activation inhibits expression of proinflammatory mediators through downregulation of PI3K/p38 MAPK and NF-κB signaling in murine macrophages. *DNA Cell Biol*. 2015;34(2):133–141. doi:10.1089/dna.2014.2630
49. Zhang Z, Wang S, Zhou S, et al. Sulforaphane prevents the development of cardiomyopathy in type 2 diabetic mice probably by reversing oxidative stress-induced inhibition of LKB1/AMPK pathway. *J Mol Cell Cardiol*. 2014;77:42–52. doi:10.1016/j.yjmcc.2014.09.022
50. Li X, Wu D, Tian Y. Fibroblast growth factor 19 protects the heart from oxidative stress-induced diabetic cardiomyopathy via activation of AMPK/Nrf2/HO-1 pathway. *Biochem Biophys Res Commun*. 2018;502(1):62–68. doi:10.1016/j.bbrc.2018.05.121
51. Peng M, Qiang L, Xu Y, Li C, Li T, Wang J. Inhibition of JNK and activation of the AMPK-Nrf2 axis by corosolic acid suppress osteolysis and oxidative stress. *Nitric Oxide*. 2019;82:12–24. doi:10.1016/j.niox.2018.11.002
52. Xiong GF, Li DW, Zheng MB, Liu SC. The effects of Lycium Barbarum Polysaccharide (LBP) in a mouse model of cerulein-induced acute pancreatitis. *Med Sci Monit*. 2019;25:3880–3886. doi:10.12659/msm.913820